ASTRONOMY & ASTROPHYSICS
SUPPLEMENT SERIES

Astron. Astrophys. Suppl. Ser. **108,** 279-285 (1994)

A spaceborne near-Earth asteroid detection system

B.V. Jackson[1], A. Buffington[1], P.L. Hick[1], S.W. Kahler[2] and D.F. Webb[3]

[1] Center for Astrophysics and Space Sciences, San Diego, California 92093, U.S.A.
[2] Phillips Laboratory/GPSG, Hanscom AFB, Massachusetts 01731, U.S.A.
[3] Institute for Space Research, Boston College, Newton Center, Massachusetts 02159, U.S.A.

Received September 21, 1993; accepted April 20, 1994

Abstract. — We have designed a Solar Mass Ejection Imager (SMEI) to image transient heliospheric features from Earth orbit over the entire sky every 90 minutes. The instrument is designed to detect changes on this time scale in the signals from sunlight Thomson-scattered from electrons at a brightness level of tenth magnitude per square degree of sky. We explore the possibility of using such an instrument to detect asteroids passing near the Earth. We estimate that SMEI will detect at least 13 asteroids per year over ~12 m in radius.

Key words: instrumentation: photometers — methods: data analysis — meteoroids — minor planets

1. Introduction

In recent years, we have used the zodiacal light photometer experiments on the Helios spacecraft (Leinert et al. 1981) in a novel way as heliospheric coronagraphs to study solar mass ejections in the outer corona and heliosphere. Analogous to coronagraphs, the photometers detect solar white-light radiation Thomson-scattered from free electrons in the interplanetary plasma. This technique of imaging a large portion of the inner heliosphere with Helios photometer data (Jackson & Leinert 1985) has been used to determine the brightnesses, numbers, temporal variations, speeds and spatial distributions of large-scale features propagating through the heliosphere. These features include solar mass ejections (Jackson 1985; Jackson et al. 1985; Webb & Jackson 1990), coronal streamers (Jackson 1991), interplanetary shock waves (Jackson 1986), and comets (Jackson & Benensohn 1990).

These results have led to a proposal for an improved experiment, the Solar Mass Ejection Imager (SMEI), to image solar mass ejections and other heliospheric features from Earth orbit and detect their motion toward the Earth (Jackson et al. 1989, 1991, 1992). This experiment, designed to observe large-scale differences in brightness over the sky, consists of three electronic camera/sensor systems, each of which contains a wide-angle, fan-beam optical system. Each system is baffled to reduce stray light falling on the image plane to more than 15 orders of magnitude below direct sunlight. The off-axis mirror optical system feeds a CCD camera with images of sufficient size and uniformity to minimize the effects of the pixel-to-pixel and subpixel response gradients of the CCD detector (Buffington et al. 1991). The CCD pixels and the image size on the focal plane permit binning the sky in half-degree or larger resolution elements while still maintaining the designed signal-to-noise ratio for point sources. The optimum configuration for the experiment requires a three-axis stabilized, zenith-nadir pointing spacecraft in Earth orbit at ~800 km altitude. The sensors are rigidly mounted to the spacecraft, allowing its orbital rotation to sweep out the entire sky every 90 min. Each of the three sensors covers a different 3° × 60° field of view such that together they view a thin 180° slice of the sky. The plane of the detector slits is oriented perpendicular to the spacecraft velocity vector. Figure 1 is a schematic of this instrument in an equatorial orbit.

SMEI is designed to detect changes in sky brightness at the level of one S10 unit (the equivalent of a tenth magnitude star in one square degree of sky) at 90° elongation from the Sun-Earth line. The advantage of SMEI as an asteroid detection system is that it views nearly the entire sky each 90-minute orbit. This implies that over a period of time SMEI will be able to determine the number of asteroids within a limited size range passing near the Earth. Once asteroids are detected and their orbital parameters determined to first order by SMEI, they can be tracked by more sophisticated ground-based instruments to determine more accurately their orbital parameters. Since all of the large asteroids SMEI will observe come close to the Earth, they all are in potentially dangerous Earth-crossing orbits.

In the next section we describe the detection capabilities of SMEI for near-Earth asteroids with typical albedos, sizes and speeds. We then determine the expected rates

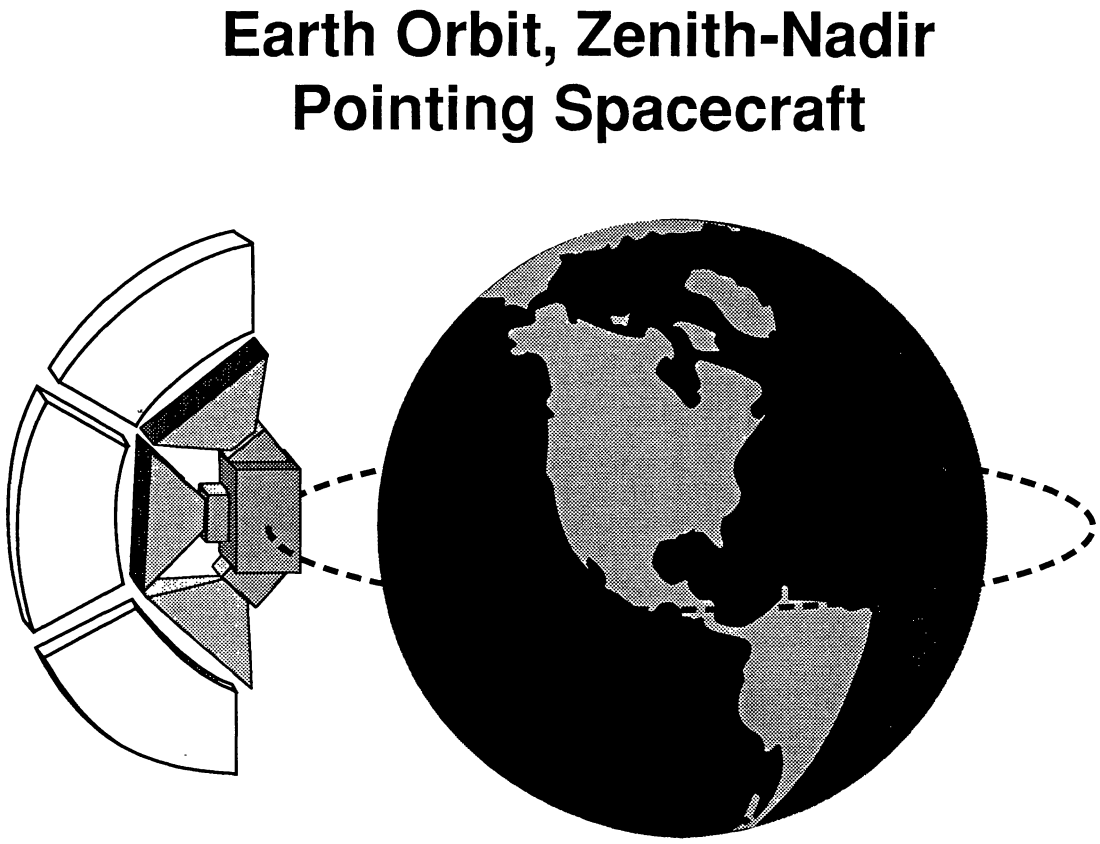

Fig. 1. Schematic of the SMEI experiment in an equatorial Earth orbit. The spacecraft orbit is circular at ≈800 km above the surface of the Earth. Three camera heads view the sky in a narrow fan beam 180° wide, scanning perpendicular to the spacecraft orbital motion

for asteroid detections as functions of their size based on the empirical flux distribution of objects at the top of the atmosphere from Hughes (1992). This is followed by a discussion of the detection of smaller bodies by observation of streaks in individual images. In the last two sections we discuss modifications to the analysis which could enhance our ability to detect these objects, and we summarize our results in terms of predictions of the numbers of asteroids that SMEI will detect per year.

2. Detection capabilities for near-Earth asteroids

SMEI is designed to detect sky brightness changes greater than tenth magnitude. This threshold is set by the scanning rate across the sky and the detector sensitivity. The size limit to which SMEI will detect asteroids depends on the size of the asteroid, its illumination by the Sun, and its distance from the Earth. If we assume that asteroids are spherical and have no glints caused by grazing-incidence reflections, their illumination by sunlight at a given distance from the Earth is given approximately by the formula

$$M_\epsilon - M_{180} = -2.5 \log \left[\sin^2 \left(\frac{\epsilon}{2} \right) \right], \qquad (1)$$

where M_ϵ is the magnitude of the asteroid at a solar elongation angle ϵ, and M_{180} is its magnitude at $\epsilon = 180°$, where it is fully illuminated. The instrument will not be able to view closer than within 18° of the Sun because of the design limiting stray light on the detectors. We note that SMEI is designed to have a signal-to-noise ratio for a one S10 signal no worse than 3σ at an elongation angle of 90°. Closer to the Sun, the rapid increase of the zodiacal light brightness increases the noise for point-like signals. Although this noise increase has not been included in our calculations, we estimate that it will have little effect on the number of asteroids observed by SMEI.

The magnitude M_{180} of an asteroid depends on its albedo, distance from the Earth and size as given in the following equation

$$M_{180} - M_0 = -2.5 \log \left[\frac{P}{P_0} \times \left(\frac{D_0}{D} \right)^2 \times \left(\frac{R}{R_0} \right)^2 \right], \qquad (2)$$

where M_0 is the magnitude of a calibrated source, $\frac{P}{P_0}$ is the ratio of the asteroid and calibrator albedos, $\frac{D_0}{D}$ is the ratio of the calibrator and asteroid distances, and $\frac{R}{R_0}$ is the ratio of the asteroid and calibrator radii. Because we

expect to observe only those asteroids near Earth at 1 AU, a factor relating their distance from the Sun is not included in Eq. (2). The full Moon ($M_0 = -12.7$) has a geometric albedo of 0.11 and a radius of 1738 km (Allen 1976). If we use the Moon as the calibrator and determine all measurements relative to this, Eq. (2) reduces to

$$M_{180} = 7.2 - 2.5 \log \left[P \left(\frac{R}{D} \right)^2 \right], \quad (3)$$

where P is the geometric albedo, D is the distance in Earth radii ($R_E = 6.37\ 10^3$ km), and R is the radius in meters. Combining Eqs. (1) and (3) and solving the resulting equation for D for a limiting $M_\epsilon = 10$ object, we get:

$$D = 3.63\, R \sin \left(\frac{\epsilon}{2} \right) \sqrt{P}. \quad (4)$$

We find that an asteroid 100 m in radius with an albedo of 0.15, values typical of many near-Earth asteroids (e.g., Shoemaker et al. 1979; McFadden et al. 1989) could, at 180° elongation, be observed out to a distance of 140 R_E, or 2.3 times the distance from the Earth to the Moon. Figure 2 depicts the area within which SMEI will detect at tenth magnitude an asteroid of 100 m radius. SMEI will view a volume of space delineated by this area rotated about the Sun-Earth line. As is evident from the figure, detections of asteroids will be more likely in the hemisphere opposite the Sun.

Objects passing near the Earth are detected by their motions relative to the background on either individual exposures or consecutive maps of the same area of the sky. Using the SMEI observations, we will assemble a map of the entire sky on each orbit from which we will obtain difference maps. These difference maps will then be used to search for moving objects. As an asteroid moves across the sky, it will be detected as a line of anomalously bright resolution elements ("points") in consecutive maps. In the next two sections, we describe two methods for estimating the number of near-Earth objects which SMEI will be able to detect. The first is based on detecting larger objects (asteroids) as points which have moved between consecutive sky maps. The second method is based on detecting smaller objects as streaks during individual exposures on a single orbit.

3. Estimated detection rate of asteroids

To determine the detection rate for asteroids by SMEI, we must combine the detection limits of the instrument with the estimated numbers of asteroids that come near the Earth. Shoemaker et al. (1979) have estimated that 1300 to 2500 Earth-crossing asteroids brighter than an absolute magnitude of 18 (at 1 AU) may exist. About 140 objects which cross the orbit of the Earth are known today (e.g., Morrison 1992). About 20–40% of all Earth-crossing asteroids remain in these orbits long enough to impact the Earth; a recent estimate is that there are about 2000 Earth-crossing asteroids with diameters ≥1 km (Morrison 1992).

Hughes (1992) presented a graph showing the numbers of objects incident upon the Earth. The cross-sectional area over which such objects can be observed by SMEI is considerably greater than that of the Earth. We use Hughes' empirical data to estimate the expected numbers of objects detectable by SMEI as a function of size. As summarized by Hughes (1992), the integral number flux of meteorites incident at the top of the Earth's atmosphere per year versus mass can be approximated by a straight line on a log-log plot (Hughes' Fig. 2). The mass of the largest meteorite that strikes the Earth once per year is $\sim 10^9$ g. Assuming a specific gravity of 3 g cm^{-3}, this meteorite contains 3.3 10^8 cm^3 of material and has a radius of 4.3 m (see Eq. (7) below). An asteroid with 400 times this mass has a radius of 32 m. An asteroid of this size or larger, on average, should strike the Earth only once every 500 years. The Tunguska object which fell early this century was about this size (Hills & Goda 1993). By this method of calculation, an asteroid of a size expected to hit only once in 10^6 yr (Kresák 1978) has a radius >400 m and would create a crater 20 km in diameter when it hits the Earth. The asteroid now thought to have caused the mass extinctions 65 million yr ago at the Cretaceous-Tertiary boundary was about ten times larger in radius (Morrison 1992).

The number of objects which SMEI can detect is estimated in the following way. First, we differentiate the Hughes curve to convert from integral number flux above a given mass to differential number flux per mass interval. We then convert the plot to differential number flux as a function of size (radius) instead of mass. This differential function is then multiplied by an areal function to account for the larger cross-sectional detection area swept out by SMEI. Finally, we integrate the SMEI differential detection distribution to return to an integral number distribution.

We write the Hughes function as

$$N_{>M} = 10^{8.94}\, M^{-1}, \quad (5)$$

where $N_{>M}$ is the number of asteroids per year above a given mass M in grams. The derivative of the Hughes function is

$$\frac{dN}{dM} = 10^{8.94}\, M^{-2}. \quad (6)$$

The mass of an asteroid is

$$M = \rho \frac{4}{3} \pi R^3, \quad (7)$$

so

$$dM = \rho 4\pi R^2 \, dR. \tag{8}$$

For a specific gravity of 3 g cm^{-3}, substituting Eqs. (7) and (8) into (6) we obtain

$$\frac{dN}{dR} = 208 R^{-4}, \tag{9}$$

which is the differential number distribution as a function of asteroid radius in meters.

To convert this number, which is that impinging on the Earth, to the number observed by SMEI, we must multiply Eq. (9) by the ratio of the area swept out by SMEI (Fig. 2) to the area of the Earth. The volume of space viewed by SMEI approximates a sphere not centered on the Earth with a radius r (in R_E) that is roughly three-fourths of the distance given in Eq. (4) at 180° elongation or

$$r = 2.72 R\sqrt{P}. \tag{10}$$

The more observations that can be obtained of the object within the volume, the more certain we will be that an asteroid has moved across the sky and the better we can determine its orbit. Speeds of near-Earth objects relative to the Earth range from 12 to 30 km s^{-1} with a peak at ~15 km s^{-1} (Hughes 1992; Rabinowitz 1993). As a limit for a minimum detection we assume that an asteroid must be observed at tenth magnitude or brighter moving along a relatively straight line in at least three consecutive sky maps. Assuming a speed of 15 km s^{-1}, an asteroid will travel 25 R_E between the first and third observations. In the limiting case for detections, an asteroid will travel only this distance within the observing volume. The limiting case for a 100 m asteroid is shown in Fig. 2. The distance to this asteroid at its closest approach to the center of the observing volume determines the approximate SMEI cross-sectional area for an asteroid detection. The modified Eq. (10) is

$$r^2 = 1.11 R^2 - 12.5^2, \tag{11}$$

where we assume $P = 0.15$. The SMEI differential distribution is then obtained by multiplying Eq. (9) by (11) to get

$$\frac{dN}{dR} = 231 R^{-2} - 3.25\ 10^4 R^{-4}. \tag{12}$$

Integrating Eq. (12) yields the integral distribution

$$N_{>R} = 231 R^{-1} - 1.08\ 10^4 R^{-3}. \tag{13}$$

Figure 3 shows this integral number distribution versus radius for objects that we expect to observe with SMEI. For the point method, Eq. (13) yields the result shown by the linear solid line in the upper right of the figure ("HUGHES"). Note that Eq. (12) implies that the smallest observable asteroid is 12 m in radius and must travel

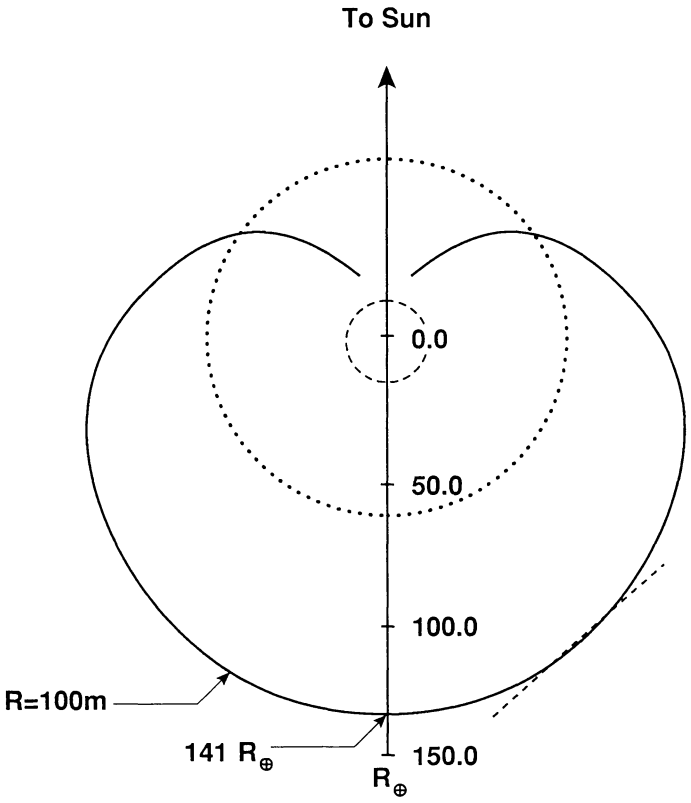

Fig. 2. An example of the detection area of SMEI. The solid line is the cross-sectional area of space within which SMEI can detect asteroids with a radius of 100 m and a geometric albedo of 0.15 (Eq. (4)). The distance scale is given in Earth radii (R_E). The orbit of the Moon is shown as the dotted circle. The approximate inner limit of the point method for small asteroids imposed by asteroid motion is depicted as the inner dashed circle. The straight dashed line in the lower right of the figure shows a typical trajectory of a 100 m asteroid which travels 25 R_E within the observing volume in the limiting case

directly through the center of the volume. The calculation shows that SMEI will observe about 13 asteroids of greater than 12 m radius each year. According to Hughes (1992), asteroids of this size or greater hit the Earth once every ~30 yr. We estimate that each year SMEI should observe approximately 7 asteroids exceeding the 32 m radius of the Tunguska object.

For the rates of larger asteroids, Hughes includes the numbers of asteroids of large mass derived from the cratering observations of Morrison & Chapman (1990). In comparison with the extension of the Hughes plot given by Eq. (5), the Morrison and Chapman curve is flatter, implying a higher rate for large asteroids as shown by the dashed line at the bottom of Fig. 3. An approximation of the Morrison & Chapman (1990) curve can be made by replacing Eq. (5) with an $M^{-2/3}$ function. In this case, Eq. (12) is proportional to R^{-1} for asteroids with radii >32 m. Integration of the modified Eq. (12) diverges for infinite R and results in an equation proportional to ln

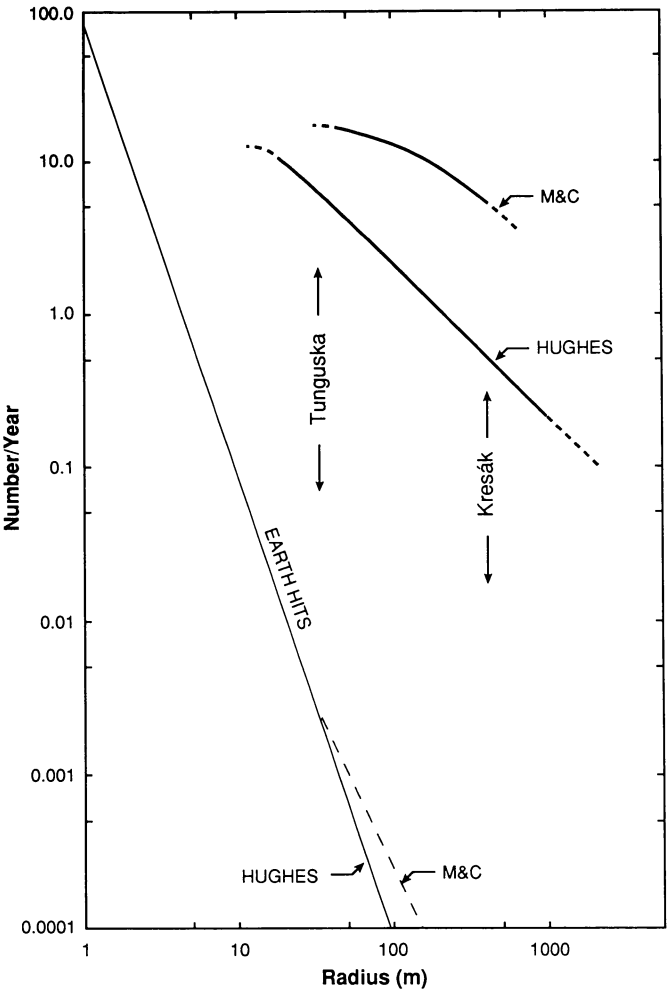

Fig. 3. Expected integral number of objects detected per year by SMEI from Earth orbit, plotted versus asteroid radius (upper bold curves). It is assumed that SMEI can detect asteroids to tenth magnitude and that all have an albedo of 0.15. The line labeled "Earth Hits" is the original Hughes (1992) function for the empirically derived meteor flux impinging on the Earth, converted from mass to radius distributions ("Hughes"). We also have calculated the impact and detection rates based on Morrison & Chapman's (1990) data as plotted by Hughes ("M&C")

(R). The Morrison and Chapman curve in Hughes (1992) suggests that asteroids with masses of about 10^{15} g are ten times more numerous than those given by the Hughes M^{-1} function. With this assumption we derive the curved plot in the upper right of Fig. 3 ("M&C"). These data imply that SMEI should observe about 17 asteroids greater than ~32 m radius each year. The Morrison and Chapman power law for large asteroids has recently been confirmed by Ceplecha (1992) and Rabinowitz (1993) from observations of near-Earth asteroids by the Spacewatch telescope.

4. Estimated detection rate for objects which cause streaks

Objects such as meteoroids which are close to the Earth move from one resolution element to another within a single image because of their rapid motion. Since the object produces a streak in the SMEI image, this can be used to distinguish it from stars. Note that these streaks result from the motion of an object in space near the Earth and are not related to the streaks produced by the ablation of objects entering the atmosphere (i.e., "meteors"). The average relative motion to Earth of 15 km s^{-1} for these objects implies a median value of the proper motion for them of ~13 km s^{-1} assuming a random direction distribution. We define n as the number of image resolution elements in the streak, where the basic resolution element is 1 deg^2. If we assume an angular speed in the SMEI field of view of $n/48$ s, the basic SMEI integration time, and a proper motion of 13 km s^{-1}, the relation between n and r_E, the distance to the meteoroid in R_E, is

$$n = 5.5\, r_E^{-1}. \tag{14}$$

The shortest detectable streak produced by a meteoroid covers 2 image resolution elements, so that the maximum distance to which the meteoroid can be observed is $r_E = 2.8\, R_E$. To retain the 3σ sensitivity, a streak produced by the meteoroid of $n \geq 2$ resolution elements dictates that the limiting tenth magnitude brightness requirement for the object given by Eq. (10) must be increased by a factor of n. This modified requirement is given by

$$r_E = \frac{2.72\sqrt{P}\,R}{\sqrt{n}}, \tag{15}$$

and

$$r_E = \frac{2.72\sqrt{P}\,R\sqrt{r_E}}{\sqrt{5.5}}, \tag{16}$$

which, for $P = 0.15$, becomes

$$r_E = 0.20\, R^2. \tag{17}$$

Therefore, at the limiting distance of 2.8 R_E, the radius of the smallest object detectable by the streak method is ~4 m. However, below 5 m radius, the numbers of artificial satellites and space debris in orbit near Earth become significantly larger than the numbers of meteoroids by several orders of magnitude (Johnson & McKnight 1987). Because of their average relative motion (~10 km s^{-1}) and proximity to the SMEI orbit, most space debris that is observed will produce streaks in the images. By integrating the numbers of space debris by their average locations and sizes (Johnson & McKnight 1987), we find that SMEI could observe several of these objects per orbit, depending on the assumed albedo. Most of these objects will have radii in the range of 0.1 to 0.5 m and be indistinguishable from meteoroids in SMEI images. Thus, the amount of

space debris would greatly exceed the number of meteoroids observed as streaks.

5. Discussion

The longer a SMEI-type instrument is operational, the more objects it will detect and the better we can characterize the population of Earth-crossing objects. Our results are based on reasonable estimates of the numbers of near-Earth objects we expect to detect. Below we describe several factors which could modify our number estimates, in some cases permitting detection of even larger numbers of objects.

By developing more sophisticated algorithms specifically used to detect point sources, we might be able to significantly increase the number of near-Earth asteroids detected by SMEI. The photometric goal of SMEI is at least a 3σ detection of brightness changes at a limit of tenth magnitude over one square degree of sky during a 48 s integration time at 90° elongation. The brightness of an asteroid, which will typically be at the low end of the size distribution, can become significantly greater than tenth magnitude as it crosses the observing volume. If the object is observed on at least three consecutive orbits, we should have no problem identifying it as an asteroid. However, larger asteroids which cross near the limits of their observing volumes must be detected on more than three consecutive orbits to assure that their signals can be discriminated from random brightness fluctuations. The zodiacal light brightness over the anti-solar hemisphere (elongations >90°) is somewhat lower than that assumed in calculating the maximum observing distances in Eq. (4). This means that SMEI should observe most objects at distances greater than those given by Eq. (4) to a 3σ level. In addition, the use of smaller image resolution elements could improve the photometry for asteroids because it could significantly enhance our ability to observe such objects fainter than tenth magnitude. For instance, in the SMEI design the smallest image resolution element covers an area of approximately 1/4 of a square degree. This may allow us to observe point-like objects on successive orbits to brightness levels two times fainter than the present photometric limit. This, in turn, would double the area over which SMEI could detect a given asteroid and, therefore, would double the number of asteroids detected each year.

It would be advantageous for the data to be processed in near real-time so that possible detections could be certified by ground-based instruments. By coordinating its operations with one or more ground-based observatories, or radar installations, possible detections of asteroids by SMEI could be confirmed within a few hours and more precise orbits determined. Optically this would be especially advantageous for the larger objects which remain relatively bright (>15th mag.) near Earth for several nights. This procedure would also minimize the chances of false detections by SMEI and could be used to improve selection criteria, especially for smaller asteroids.

In our approximations we have used an average value of 0.15 for the geometric albedo of asteroids. However, the distribution of near-Earth object albedos are very uncertain. For instance, McFadden et al. (1989) indicate that the average albedo of near-Earth asteroids is about 0.2 and a few near-Earth asteroids have albedos as high as 0.5. Asteroids with an albedo of 0.5 could be observed by SMEI over an area that is $0.5/0.15 = 3.3$ times as large as given in the above analysis. If all asteroids had albedos of 0.5, SMEI could observe over 40 objects 12 m or larger every year. On the other hand, Shoemaker et al. (1979) and McFadden et al. (1989) suggest that the known Earth-crossing asteroids are brighter due to selection effects and that the majority of Earth-crossing asteroids of any size may have low albedos. A large range or skew in the albedo distribution of these asteroids could significantly alter the total number distribution estimated here.

6. Conclusions

We have demonstrated that the proposed Solar Mass Ejection Imager, which images the entire sky approximately every 90 min, can detect asteroids passing close to the Earth. This instrument is designed to detect transient features to a brightness level of tenth magnitude with 3σ photometric accuracy per square degree of sky at $\geq 90°$ elongation from the Sun. The distance to which SMEI will be able to detect asteroids is a function of the size of the object and its brightness. For example, SMEI will observe asteroids with an albedo of 0.15 and radii $\geq$100 m to a distance of 140 R_E, at the rate of one yr^{-1} based on the Hughes distribution.

In summary, we find that SMEI will detect about 13 asteroids per year $\geq$12 m in radius of which 7 are $\geq$32 m in radius based on the Hughes (1992) number distribution. However, based on the results of Morrison & Chapman (1990) and Rabinowitz (1993) the latter rate becomes 17 asteroids per year $\geq$32 m in radius. In addition, SMEI will detect numerous small objects (mostly space debris) as streaks in the images.

Acknowledgements. Our work has been supported at the University of California at San Diego by USRA contract 6115-04, and at Boston College by the Air Force Phillips Laboratory/GPS under contract AF19628–90–K–0006.

References

Allen C.W. 1976, Astrophysical Quantities 3rd edition (Athlone Press, London) 144
Buffington A., Booth C.H., Hudson. H.S. 1991, PASP 103, 685
Ceplecha Z. 1992, A&A 263, 361
Hills J.G., Goda M.P. 1993, AJ 105, 1114

Hughes D.W. 1992, Space Sci. Rev. 61, 275
Jackson B.V. 1985, Solar Phys. 100, 563
Jackson B.V. 1986, Adv. in Space Res. 6, 307
Jackson B.V. 1991, J. Geophys. Res. 96, 11307
Jackson B.V., Leinert C. 1985, J. Geophys. Res. 90, 10759
Jackson B.V., Benensohn R.M. 1990, Earth, Moon and Planets 48, 139
Jackson B.V., Howard R.A., Sheeley N.R. Jr. et al. 1985, J. Geophys. Res. 90, 5075
Jackson B.V., Hudson H.S., Nichols J.D., Gold R.E. 1989, eds. J.H. Waite Jr., J.L. Burch, R.L. Moore, Solar System Plasma Physics Geophysical Monograph 54. AGU, Washington, 287
Jackson B., Gold R., Altrock R. 1991, Adv. Space Res. 11, 377
Jackson B.V., Webb D.F., Altrock R.C., Gold R. 1992, eds. Z. Svestka, B.V. Jackson, M.E. Machado, Lecture Notes in Physics 399, Eruptive Solar Flares (Springer-Verlag, Heidelberg) 322
Johnson N.L., McKnight D.S. 1987, Artificial Space Debris (Orbit Books, New York)
Kresák L. 1978, Bull. Astron. Inst. Czech. 29, 114
Leinert C., Pitz E., Link H., Salm N. 1981, Space Sci. Instrum. 5, 257
McFadden L.A., Tholen D.J., Veeder G.J. 1989, Physical properties of Aten, Apollo and Amor asteroids, eds. R.P. Binzel, T. Gehrels, M.S. Matthews, Asteroids II (The University of Arizona Press, Tucson) 442
Morrison D. 1992, The Spaceguard Survey: Report of the NASA International Near-Earth-Object Detection Workshop (NASA JPL, Pasadena, CA)
Morrison D., Chapman C.R. 1990, Sky and Telesc. 79, 261
Rabinowitz D.L. 1993, ApJ 407, 412
Shoemaker E.M., Williams J.G., Helin E.F., Wolfe R.F. 1979, Earth-crossing asteroids: orbital classes, collision rates with Earth, and origin, ed. T. Gehrels, Asteroids (The University of Arizona Press, Tucson) 253
Webb D.F., Jackson B.V. 1990, J. Geophys. Res. 95, 20641